Statistical modeling of enamel rater value data

Isogai, Takafumi
Uchida, Hiroaki
Miyama, Susumu
Nishiyama, Sadao

(Citation)
Journal of Applied Statistics,35(5):515-535

(Issue Date)
2008-05

(Resource Type)
journal article

(Version)
Accepted Manuscript

(URL)
https://hdl.handle.net/20.500.14094/90000774

Statistical Modeling of Enamel Rater Value Data

Takafumi Isogai[*], **Hiroaki Uchida**[**], **Susumu Miyama**[***] & **Sadao Nishiyama**[****]

[*] *Faculty of Maritime Sciences, Kobe University, Japan,*

[**] *Technology and Development Division, Universal Can Corporation, Japan,*

[***] *Technical Development Center, Mitsubishi Aluminium Co., Ltd, Japan,*

[****] *Technology and Development Division, Universal Can Corporation, Japan*

Abstract

Enamel Rater Value (shortly, ERV) of a quick stress test is usually used to evaluate the integrity of an organic coating for the inside of an aluminium (denoted by Al shortly) can. A large positive value of ERV is supposed to indicate the degree of imperfect coating coverage, i.e. the size of an exposed Al area. An Al can filled with some drink, if there is an exposed Al area due to imperfect coating coverage, has Al dissolution brought by corrosion. Thus a smaller value of ERV is desirable to prevent Al dissolution. However, quantitative evaluations of ERV data as well as an accumulated quantity of Al dissolution have never been published, because ERV is involved in complicated anode dissolution of an exposed Al area. Recently our experimental study has found out a relationship between ERV and sizes of exposed Al areas. This relationship enables us to construct a descriptive statistical model for ERV data as well as to evaluate coating effects for Al cans. Furthermore, empirical implications suggest that an instantaneous quantity of Al dissolution is proportional to ERV. Using this fact we can derive a predictive statistical model for an accumulated quantity of Al dissolution in an Al can.

Keywords: Enamel Rater Value, aluminium cans, corrosion, aluminium dissolution, generalized Gamma distribution, new power normal family

Introduction

Aluminiun (denoted by Al shortly) beverage cans are very popular in our modern life. The insides of such Al beverage cans are usually covered with various organic coatings to maintain an acceptable shelf life (e.g. Nishiyama (1988)). The coating integrity is evaluated by so-called Enamel Rater Value (shortly, ERV) of a quick electrical stress test (Lopez (1987) p.91). ERV measures an instantaneous electric current between the body of an Al can (i.e. anode) and a stainless stick (i.e. cathode), just after an Al can filled with 1% brine has been energized with 6.2 voltage for four seconds. The magnitude of ERV is supposed to indicate the degree of imperfect coating, i.e. the size of an exposed or nearly exposed Al area due to imperfect coating, which we call a defective area hereafter. In an Al can filled with some drink, if there is a defective area, corrosion will happen as time is passing, and it ordinarily brings Al dissolution. Thus a smaller value of ERV is desirable to prevent Al dissolution.

Owing to simplicity of ERV measurement, ERV is usually utilized in a manufacturing process of Al cans to detect abnormalities of the process. On the other hand, ERV is involved in a complex phenomenon due to anode dissolution of a defective area (for criticism of ERV, see, e.g., Nishiyama et al. (1994)). Therefore, it is difficult to find reports about a quantitative evaluation of ERV in the literature.

Our objective here is to construct not only a descriptive statistical model for ERV data of Al cans coming from an ordinary manufacturing process under control but also a predictive statistical model for an accumulated quantity of Al dissolution brought by corrosion in an Al can.

We first experimentally examine the relationship between ERV and the size of a defective area. It is turned out that ERV is expressed as a power function of the size of an exposed Al area. Using this relationship, we can construct a descriptive model for ERV data, which enables us to evaluate coating effects for Al cans. Furthermore, empirical implications suggest that an instantaneous quantity of Al dissolution is proportional to ERV. Thus, by use of this fact we can construct a predictive model for an accumulated quantity of Al dissolution. Performance of our predictive model for an accumulated quantity of Al dissolution is evaluated through data sets of accelerated life tests.

Examination of a relationship between ERV and the size of a defective area

In ERV measurement the body of an Al can is treated as anode. So, when an electric current starts to run in measuring ERV, if there is a defective area, the progress of electro-chemical reaction over the defective area causes a dissolution of aluminium ions

(i.e. Al dissolution), which generates pits. Two cases of fluctuations of ERV are expected. One is the case where a frequency of occurrence of pits may change according to sizes of defective areas. The other is the case where electro-chemical differences may arise in patterns of Al dissolution as time is passing, and electric currents have violent oscillations. Thus, the following experiment was performed to evaluate fluctuations of ERV due to different sizes of defective areas as well as time-dependent fluctuations of ERV.

In our experimental study exposed Al areas of Al pieces were treated as defective areas. Table 1 shows combinations of sizes of defective areas, unit defective areas and the number of unit defective areas, which is defined as a ratio of the size of a defective area to a unit defective area. For the sake of simplicity, in Table 1 and also in the following we denote the size of a defective area, the size of a unit defective area and the number of unit defective areas by a defect size, a unit defect size and a defect count respectively.

The smallest defect size is $0.2\,\mathrm{mm}^2$ and the largest one is $20\,\mathrm{mm}^2$. The smallest unit defect size is $0.0314\,\mathrm{mm}^2$ and the second one is $0.0628\,\mathrm{mm}^2$. The word 'All' in Table 1 means the case where a defect size itself is a unit one. Our interest is in whether or not different unit defect sizes bring time-dependent variations with respect to ERV. By making use of Al pieces with exposed Al areas, of which sizes are the same defect sizes in Table 1, ERV was measured two or three times repeatedly according to a combination of each unit defect size and a defect count. The measurement was continuously done every 10 milli-seconds in the span of 10 seconds.

Table 1

Inquiry about time-dependent variations in ERV measurement

To examine time-dependent variations of ERV, correlation analyses were carried out. Figure 1 gives scatter plots between ordinary ERV versus the average ERV's, of which time span is one second, two seconds, four seconds or ten seconds.

To our surprise there is no difference between two scatter plots of ordinary ERV versus the one and ten seconds average ERV's, which means that the behavior of ERV is constant at an early stage of ERV measurement. Thus we need not take account of situations where different unit defect sizes cause time-dependent variations. In the subsequent sections we use ordinary ERV as typical ERV.

Figure 1

Statistical analysis of ERV data in our experimental study

To examine a relationship between ERV and defect sizes, Figure 2 shows two scatter plots, which are ERV versus defect sizes and also ERV divided by the corresponding defect count (denoted by ERV/(defect count), shortly) versus unit defect sizes.

Figure 2

From Figure 2 we may suppose two relationships between ERV and defect sizes, and between ERV/(defect count) and unit defect sizes as

$$ERV \propto (defect\ size)^{\tau_1}, \tag{1}$$

$$ERV/(defect\ count) \propto (unit\ defect\ size)^{\tau_2}. \tag{2}$$

As for statistical models with respect to ERV and ERV/(defect count) we take up an ordinary normal error model, and also consider a power normal family (Box & Cox (1964)), because non-normality may appear in errors. Let us denote an observed ERV by a random variable X, the distribution function of a normal by $F_N(x)$ and the distribution function of a modified Box & Cox power normal family by $F_{MP}(x)$. Then $F_N(x)$ and $F_{MP}(x)$ are given by

$$F_N(x) = \Phi\left(\frac{x-\eta}{\sigma}\right) \quad (\sigma > 0) \tag{3}$$

$$F_{MP}(x) = \Phi\left(\frac{1}{\sigma}\left\{\frac{(x/\eta)^{\lambda}-1}{\lambda}\right\}\right) \quad (\sigma > 0), \tag{4}$$

where Φ is the distribution function of the standard normal distribution.

In models (3) and (4) we supposed

$$\eta = e^{\alpha_1}(defect\ size)^{\tau_1} \tag{5}$$

as a regression structure for ERV, and analyzed ERV data obtained under the conditions of Table 1. The results are given in Table 2. From Table 2 we see that there is some difference in the degree of goodness-of-fit with two models (3) and (4). To examine their degrees of goodness-of-fit, in Figure 3 we show two normal probability plots with residuals

$$\hat{r} = \frac{x - \hat{\eta}}{\hat{\sigma}} \quad \text{and} \quad \hat{e} = \frac{1}{\hat{\sigma}} \left\{ \frac{\left(x / \hat{\eta} \right)^{\hat{\lambda}} - 1}{\hat{\lambda}} \right\}.$$

In 5% significance level Shapiro-Wilk test accepts the hypothesis of normality for the residual of the modified Box & Cox family, and rejects normality for the residual of the normal error model.

Table 2
Figure 3
Table 3
Figure 4

Similar analysis for ERV/(defect count) was carried out with relation to the following regression structure

$$\eta = e^{\alpha_2} \left(unit\ defect\ size \right)^{\tau_2}. \tag{6}$$

The results are given in Table 3 and Figure 4. Table 3 shows that there is a large difference in the degree of goodness-of-fit with two models (3) and (4). In 5% significance level Shapiro-Wilk test accepts the hypothesis of normality for the residual of the modified Box & Cox family, and rejects normality for the residual of the normal error model.

Finally we remark that the usual Box & Cox power normal family with a location parameter fits ERV well, but does not fit ERV/(defect count) at all. Because in reality we can know neither a defect count nor a unit defect size beforehand, on the average we may suppose

$$ERV \propto \left(defect\ size \right)^{\tau} \tag{7}$$

as a relationship between ERV and the size of a defective area.

Relationship between ERV and the instantaneous quantity of Al dissolution

Here, based on our experimental results, we consider a relationship between ERV and the quantity of Al dissolution. As is well known, when defect sizes, i.e. sizes of exposed Al areas are not too small, aluminium ions do not dissolve from the whole surface of an exposed Al area, but it dissolves from pits caused by electro-chemical partial attacks, what is called occurrence of corrosion. Once a pit begins to grow, hydroxide arises around the pit due to the development of corrosion and it covers the pit after a while.

During this process another pit appears one after another over the rest exposed Al area, and it comes to an end in the same way.

Combining the above response process with our experimental result that ERV is constant over ten seconds, we may suppose that neither occurrence nor shut-off rates of pits have time-dependent variations, and that they are constant during such a short period. This means that with regard to an exposed Al area the instantaneous quantity of Al dissolution caused by pits are constant over ten seconds. Thus, if pits with Al dissolution exist at a constant rate for a unit defective area, the instantaneous quantity of Al dissolution (i.e. Al dissolution rate) becomes proportional to ERV. We call such pits with Al dissolution and their total size as active pits and an active pitting size respectively, and put a proportionality factor of the active pitting size as Q.

The existence of such a proportional relationship has been indicated by one of the authors in a report of the experiment held at Fuji-Oyama Japanese factory in 1982. That is, the relation

$$(Al\ dissolution\ rate) \propto ERV \tag{8}$$

holds. Also we have

$$(active\ pitting\ size) = Q \times (defect\ size). \tag{9}$$

Using the relationship (7), from (8) and (9) we conclude that

$$ERV \propto (active\ pitting\ size)^{\tau} \tag{10}$$

and

$$(Al\ dissolution\ rate) \propto (active\ pitting\ size)^{\tau}. \tag{11}$$

Statistical model for ERV data

To construct a descriptive statistical model for ERV data, we shall use the empirical relationship (10) in the previous section, and express an unobservable *active pitting size* by an appropriate sum of random variables.

Let $D\ (\geq 0)$ denote a defect size. We suppose that if $D = 0$, ERV is zero. Also suppose that $D\ (> 0)$ is large enough to generate pits one after another in measuring ERV. Let us denote the size of an active pit by a random variable $U\ (> 0)$. When $D > 0$, in the measurement process there always exist several active pits, of which sizes are

$U_1, U_2, \ldots, U_{N(D)}$, where $N(D)$ means some counting process to indicate the number of active pits. Then, an *active pitting size* S for $D(>0)$ is expressed as

$$S = \sum_{i=1}^{N(D)} U_i \,. \tag{12}$$

Note that our initial condition leads to $N(0) = 0$. Also suppose that $N(D)$ and U_i $\left(i = 1, 2, \ldots, N(D)\right)$ are independent of each other, and that U_i's are enough small not to overlap. Then, from (10), ERV is written as

$$ERV = C(S)^{\tau} = C\left(\sum_{i=1}^{N(D)} U_i\right)^{\tau}, \tag{13}$$

where $C(>0)$ is a proportionality constant independent of *D*. From the relationship (9), we know that $Q = \sum_{i=1}^{N(D)} U_i / D$. To clarify a meaning of *Q*, we decompose Q and rewrite ERV as

$$ERV = C\left(D \cdot \frac{N(D)}{D} \cdot \frac{\sum_{i=1}^{N(D)} U_i}{N(D)}\right)^{\tau}. \tag{14}$$

From the constancy of Q we may suppose that

$$\xi = \lim_{D\to\infty} \frac{N(D)}{D}, \tag{15}$$

where a parameter $\xi(>0)$ explains an average frequency of active pits per unit area.

To derive a distribution of ERV, we need further several assumptions. Suppose that U_i's are distributed as an exponential distribution with unit scale parameter. As we cannot know the number of $N(D)$ in the factor $\sum_{i=1}^{N(D)} U_i / N(D)$, we shall treat its number as an unknown parameter *k*. Under the above assumptions, taking the logarithm of both sides of (14), we have the following approximate distribution for ERV:

$$\begin{aligned} \log ERV &= \log C + \tau \log D + \tau \log \xi + \tau \log \frac{\sum_{i=1}^{k} U_i}{k} \\ &= \varphi + \tau \log D + \sigma\sqrt{k} \log \frac{\sum_{i=1}^{k} U_i}{k}, \end{aligned} \tag{16}$$

where we put

$$\begin{aligned} \varphi &= \log C + \tau \log \xi \\ \sigma &= \tau / \sqrt{k} \,. \end{aligned} \tag{17}$$

For the sake of simplicity, let us denote ERV and $\sum_{i=1}^{k} U_i$ by X and G respectively, and put

$$\mu = \varphi + \tau \log D . \tag{18}$$

We rewrite an expression (16) of $\log ERV$ as

$$\frac{\log X - \mu}{\sigma} = \sqrt{k}\left(\log G - \log k\right). \tag{19}$$

Then, X is distributed as a generalized Gamma distribution, and the form (19) has been adopted by Lawless (1980) to examine a stable estimation for k. We add some physical meaning to the form (19) in the present paper. Especially our feature lies in an explicit expression of D in parameter μ. For another physical meaning of the form (19), see Isogai et al. (2004).

The density of X is given by

$$f_\theta(x) = \frac{k^k \left(\frac{x}{\eta}\right)^{\sqrt{k}/\sigma} \exp\left\{-k\left(\frac{x}{\eta}\right)^{\frac{1}{\sigma\sqrt{k}}}\right\}}{\sigma\sqrt{k}\,\Gamma(k)\,x}, \tag{20}$$

where we put

$$\eta = \exp\mu = D^\tau \exp\varphi \tag{21}$$

and $\theta = (\eta, \sigma, k)$. The distribution of X with (20) includes as special cases the Weibull (k=1) and the Gamma (σ=1), and also includes the Lognormal as a limiting case ($k = \infty$).

From the fact that the distribution of X with (20) is a generalized Gamma distribution, we also apply a new power normal family constructed by Isogai (1999) to ERV data, because a new power normal family approximates a generalized F distribution introduced by Prentice (1975).

The distribution function $F_{NP}(x)$ of our new power normal family is given by

$$F_{NP}(x) = \Phi\left[\frac{1}{\delta}\left\{\left(\frac{x}{\eta}\right)^{\delta/\sigma} - \exp\left(-\delta^2\right)\right\}\right], \tag{22}$$

where $-1/3 < \delta < 1/3$ and $\sigma > 0$. $F_{NP}(x)$ tends to the Lognormal as $\delta \to 0$. When $\delta \to 1/3$, it tends to the Weibull:

$$F_{NP}(x) = 1 - \exp\left(-\left(\frac{x}{\eta}\right)^{\frac{1}{\sigma}}\right),$$

and when $\delta \to -1/3$, it tends to the extreme value distribution of Type 2 (see Johnson

& Kotz (1970)):

$$F_{NP}(x) = \exp\left(-\left(\frac{x}{\eta} \right)^{-\frac{1}{\sigma}} \right) \quad .$$

In the following analysis of several data sets, we use our new power normal family (22) as a competitor against the generalized Gamma distribution (20).

Statistical distribution of ERV when a defect size $D\,(>0)$ *is known*

First we shall analyze ERV data in our experimental study mentioned before, where a defect size $D\,(>0)$ is known. We adopt two distributions, i.e. the generalized Gamma distribution (20) and our new power normal family (22) with two regression structures (5) and (6). The results are given in Tables 4 and 5.

Table 4

Table 5

In Tables 4 and 5, the value of $\hat{\delta}$ with our new power normal family exceeds its upper limit 1/3 in the model fitting, which suggests that ERV data is distributed as the Weibull. On the other hand, in case of $k=1$ (i.e. the model (20) is the Weibull) we examined the minimum value (= SSE, shortly) of the negative log-likelihood function with respect to the generalized Gamma distribution (20). Then, we have SSE = 316.59 for ERV data and the p-value of a χ^2 test statistic is p=0.0424. Also we have SSE = 174.04 for ERV/(defect count) data and the p-value of a χ^2 test statistic is p=0.560. These results indicate that ERV data is nearly distributed as the Weibull.

To check the degree of the goodness-of-fit, we examine residuals

$$\hat{r} = \frac{\log x - \hat{\mu}}{\hat{\sigma}} \quad \text{and} \quad \hat{e} = \frac{1}{\hat{\delta}} \left\{ \left(\frac{x}{\hat{\eta}} \right)^{\hat{\delta}/\hat{\sigma}} - \exp\left(-\hat{\delta}^2 \right) \right\}$$

of the model (20) and our new power normal family (22) respectively. As for the distribution of $\hat{r}$, the quantity $\hat{k}\exp\left(\hat{r}/\sqrt{\hat{k}}\right)$ is supposed to be approximately distributed as the Gamma distribution with shape parameter $\hat{k}$ under the null hypothesis, and so we give its Gamma probability plot in Figures 5 and 6. We also give a normal probability plot of $\hat{e}$ in Figures 5 and 6. From these residual plots we may suppose that ERV data is distributed as the Weibull when a defect size $D\,(>0)$ is known.

Figure 5

Figure 6

Statistical distribution of ERV when a defect size $D\ (>0)$ *is unknown*

When we try to deal with ERV data sets coming from Al cans manufactured in a stable production process under control, there two problems arise. The first one is that an Al can has two parts: its body and lid (or end). So, we need ERV data about bodies and ends of Al cans. The other one is that even if ERV data is given, sizes of defective areas are usually unknown beforehand.

Now we shall examine six investigation ERV data sets. Four of them (denoted by A(H), A(L), B(H) and B(L) hereafter) are measurements with respect to bodies of Al cans coming from two Japanese factories A and B. A use of Al bodies is for drinks of relatively high (denoted by H, briefly) or low (denoted by L) corrosiveness. The other two ERV data sets are denoted by E(H) and E(L). E(H) means ERV measurements with respect to ends of Al cans, made in Japan, for drinks of relatively high corrosiveness. E(L) means ERV data about ends, made in U.S.A., for drinks of relatively low corrosiveness. Summary statistics of those six data sets and their histograms are given in Table 6 and Figure 7 respectively.

Table 6

Figure 7

From Table 6 we know many zero values in ERV data sets of bodies of Al cans. The reason is that an ERV measuring instrument is adjusted to set ERV smaller than some threshold value K equal to zero. Thus, a proportion of zero values in ERV data can be used to evaluate the integrity of coating. The value K is given in Table 6.

Anti J- shaped histograms of all ERV data sets in Figure 7 and the relationship (7) suggest that sizes of defective areas concentrate on nearly zero values, and sometimes take large values. To describe this behavior of sizes of defective areas, we shall adopt a Gamma distribution as the statistical distribution of a defect size $D\ (>0)$.

From the result of the previous subsection, for a given defect size $D\ (>0)$ the distribution of ERV is the Weibull:

$$F_W(x) = 1 - \exp\left(-\left(\frac{x}{\eta}\right)^m\right) \tag{23}$$

where $m(>0)$ is an unknown shape parameter, and from (21) we have $\eta = D^{\tau}\exp\varphi$.

Here suppose that a random variable η^m (= T, say) has the following Gamma distribution, of which density function is defined by

$$f_G(t) = \frac{\beta^{\alpha}}{\Gamma(\alpha)} t^{\alpha-1}\exp(-\beta t) \tag{24}$$

with unknown parameters $\alpha(>0)$ and $\beta(>0)$. We call this distribution (24) a defect-size distribution. Then, the distribution function of ERV in the case of an unknown defect size $D\ (>0)$ is given by

$$\begin{aligned} F_{\theta}(x) &= \int_0^{\infty}\left\{1-\exp\left(-\frac{x^m}{t}\right)\right\} f_G(t)\,dt \\ &= 1-\frac{\beta^{\alpha}}{\Gamma(\alpha)}\int_0^{\infty} t^{\alpha-1}\exp\left(-\frac{x^m}{t}-\beta t\right)dt \end{aligned} \tag{25}$$

with unknown vector $\theta=(m,\alpha,\beta)$ $(m>0,\ \alpha>0,\ \beta>0)$. The density of $F_{\theta}(x)$ is also given by

$$f_{\theta}(x) = m x^{m-1}\frac{\beta^{\alpha}}{\Gamma(\alpha)}\int_0^{\infty} t^{\alpha-2}\exp\left(-\frac{x^m}{t}-\beta t\right)dt\,. \tag{26}$$

Examination of coating effects through six investigation ERV data sets

We cannot know whether or not zero values of ERV really appear, because true ERV smaller than some specified threshold value K is automatically recorded to be zero, which is the value of observed ERV. Thus we suppose that true ERV is positive or zero according to whether an inside coating has defects or not. Coating defects mean that there is some area left without coating, or that the whole inside coating is complete, but coating of some area is fairly thin or damaged by forming after the coating application. In these situations true ERV is supposed to be positive. On the contrary, when an inside coating has no defect, true ERV is supposed to be zero.

Now we shall introduce a binomial random variable Z such that

$$Z=0 \Leftrightarrow coating\ has\ no\ defect \Rightarrow ERV=0,$$
$$Z=1 \Leftrightarrow coating\ has\ defects \Rightarrow ERV>0$$

with $\Pr(Z=1)=p\ (>0)$ and $\Pr(Z=0)=1-p\ (>0)$. Letting true ERV denote by a random variable X, we suppose that the conditional distribution of X, given $Z=1$, is $F_{\theta}(x)$ in (25), i.e.,

$$\Pr(0<X<x\,|\,Z=1) = \int_0^x f_{\theta}(u)\,du = F_{\theta}(x),$$

and that the conditional distribution of X, given $Z=0$, is a unit distribution, that is,

$$\Pr\left(X = x \middle| Z = 0\right) = \Psi_0(x) = \begin{cases} 1 & (x = 0) \\ 0 & (x \neq 0) \end{cases}.$$

Here, letting observed ERV denote by a random variable Y, events $\{Y = 0\}$ and $\{Y > 0\}$ are expressed as

$$\{Y = 0\} = \{Z = 0\} \cup \{0 < X < K\} \quad \text{and} \quad \{Y > 0\} = \{X \geq K\}$$

respectively. Furthermore, we shall introduce a random variable Z^* such that $Z^* = 0$ indicates the event $\{Y = 0\}$ and $Z^* = 1$ indicates $\{Y > 0\}$. Then, we have

$$\Pr\left(Z^* = 0\right) = \Pr\left(Z = 0\right) + \Pr\left(0 < X < K\right)$$

$$= 1 - p + pF_\theta(K) \quad \left(= 1 - p^*, \, say\right),$$

$$\Pr\left(Z^* = 1\right) = p\left(1 - F_\theta(K)\right) \left(= p^*, \, say\right).$$

The conditional distribution of Y, given Z^*, is given by

$$\Pr\left(Y = y \middle| Z^* = 0\right) = \Psi_0(y) = \begin{cases} 1 & (y = 0) \\ 0 & (y \neq 0) \end{cases},$$

$$\Pr\left(K \leq Y \leq y \middle| Z^* = 1\right) = \int_K^y f_\theta^*(u)\, du = F_\theta^*(y),$$

where the conditional density $f_\theta^*(y)$ is defined by

$$f_\theta^*(y) = \frac{f_\theta(y)}{1 - F_\theta(K)} \quad (y \geq K). \tag{27}$$

Thus, the conditional density $h_\theta\left(y \middle| z^*\right)$ of Y, given $Z^* = z^*$, is expressed as

$$h_\theta\left(y \middle| z^*\right) = \left(\Psi_0(y)\right)^{1 - z^*} \left(f_\theta^*(y)\right)^{z^*}$$

and the density $h_\theta(y)$ of Y is given by

$$h_\theta(y) = h_\theta\left(y \middle| z^* = 0\right)\Pr\left(Z^* = 0\right) + h_\theta\left(y \middle| z^* = 1\right)\Pr\left(Z^* = 1\right).$$

For a random sample of size n, $y_1, y_2, \ldots, y_n$, we suppose that for the sake of simplicity the first n_0 of y's are zero, and the other $n_+ \left(= n - n_0\right)$ of y's are positive. Using the joint density of $y_1, y_2, \ldots, y_n$, we define its likelihood function by

$$L = \prod_{i=1}^{n} h_\theta(y_i) = \left(1 - p^*\right)^{n_0} \prod_{i=n_0+1}^{n_0+n_+} \left[p^* f_\theta^*(y_i)\right]$$

$$= \left(1 - p^*\right)^{n_0} \left(p^*\right)^{n_+} \prod_{i=n_0+1}^{n} f_\theta^*(y_i)$$

$$= \left\{1 - p\left(1 - F_\theta(K)\right)\right\}^{n_0} (p)^{n_+} \prod_{i=n_0+1}^{n} f_\theta(y_i). \tag{28}$$

Remark that if we put $p = 1$ in (28), the likelihood L becomes a censored one:

$$L = \left(F_\theta(K)\right)^{n_0} \prod_{i=n_0+1}^{n} f_\theta(y_i). \tag{29}$$

Furthermore, if $n_0 = 0$, we can put $p = 1$ from a meaning of the situation. Thus, the likelihood L becomes $\prod_{i=1}^{n} f_\theta(y_i)$. In our data sets E(H) corresponds to the case of $n_0 = 0$.

When $n_0 > 0$, the maximum likelihood estimators $\hat{\theta}$ and $\hat{p}$ with respect to (28) are obtained as solutions of the following simultaneous equations

$$p\left(1 - F_\theta(K)\right) = \frac{n_+}{n} \quad (\text{or} \quad p^* = \frac{n_+}{n}), \tag{30}$$

$$\sum_{i=n_0+1}^{n} \frac{\partial}{\partial \theta} \log f_\theta^*(y_i) = 0. \tag{31}$$

We analyzed six investigation ERV data sets. The result is shown in Table 7. Relevant probability plots are also shown in Figure 8. From values of $\hat{p}$ in Table 7 we know that A(L) apparently has a mixture distribution of $F_\theta(x)$ and $\Psi_0(x)$ with a positive mass at the origin, but the other data sets seem to have single populations of $F_\theta(x)$. From Figure 8 we also see that our statistical model (25) or (26) is adequate for ERV data sets with respect to bodies of Al cans, but not for those with respect to ends of Al cans. The reason is that Al lids tend to have small cracks in their surfaces of coating due to end making process after coating.

Table 7

Figure 8

Finally we shall consider a meaning of good coating. First of all, we need many zero values in ERV data, which means a large proportion of $1 - p^*$ or a small proportion of p^*. On the other hand, to avoid unnecessary dissolution of an organic coating, it is desirable that the thickness of coating is as thin as possible. Thus we can define an index of good coating (=IGC, shortly) by

$$IGC = \frac{p}{p^*} \tag{32}$$

$$= \frac{1}{1 - F_{\theta}(K)} . \tag{33}$$

A large value of IGC stands for a large proportion of $F_{\theta}(K)$. From (30) a simple estimate of IGC is given by

$$IGC = \frac{\hat{p}}{\hat{p}^*} = \frac{n}{n_+} \hat{p} . \tag{34}$$

Values of IGC with respect to six investigation ERV data sets are also shown in Table 7. From Table 7 we know that A(H) has the best IGC among all. The most different point of A(H) from the other is the shape of its defect-size distribution (24). The mode of the defect-size distribution of A(H) is located at the origin, but modes of defect-size distributions of the other data sets are not.

Statistical model for the accumulated quantity of Al dissolution

When we leave an Al can filled with some drink unopened for a long time, if there are defective areas (i.e. exposed or nearly exposed Al areas), electro-chemical attacks will generate pits one after another in the exposed Al areas over the elapse of time, and Al dissolution is brought by aluminium ions that dissolve from pits. We name this phenomenon Al dissolution caused by corrosion. When we open an old Al can to examine situations of Al dissolution, we can never know the history of corrosion except for the accumulated quantity of Al dissolution and the elapse of time.

In this section, to construct a predictive statistical model for the accumulated quantity of Al dissolution, we shall use the empirical relationship (11). Our idea is very simple. We regard the accumulated quantity of Al dissolution as *Al dissolution rate*, i.e. the instantaneous quantity of Al dissolution. And we replace total effects of pits, which have generated over the elapse of time and brought Al dissolution, by an *active pitting size of hypothetical pits.* Thus the elapse of time is regarded as an instantaneous stress factor in our setting.

Let $T\ (\geq 0)$ denote the elapse of time since an Al can of new products was filled with some drink, and also let $Al(T)$ denote the accumulated quantity of Al dissolution at time T. We suppose that the moment an Al can is filled with some drink, any pit does not arise, nor does Al dissolution begin (i.e. $Al(0) = 0$).

Now let us denote the size of a hypothetical active pit by a random variable $U(>0)$. Suppose that at time $T(>0)$ there appear several pits, of which sizes are $U_1, U_2, \ldots, U_{N(T)}$, where $N(T)$ means some point process to indicate the number of pits. Then, an *active pitting size* S at time $T(>0)$ is expressed as

$$S = \sum_{i=1}^{N(T)} U_i \,. \tag{35}$$

Note that our initial condition leads to $N(0) = 0$. Also suppose that $N(T)$ and U_i $\left(i = 1, 2, \ldots, N(T)\right)$ are independent of each other, and that U_i's are enough small not to overlap.

From (11), $Al(T)$ is written as

$$Al(T) = C^* (S)^{\tau} = C^* \left(\sum_{i=1}^{N(T)} U_i \right)^{\tau}, \tag{36}$$

where $C^* (> 0)$ is a proportionality constant independent of T. Here we suppose that

$$\xi^* = \lim_{T \to \infty} \frac{N(T)}{T}, \tag{37}$$

where a parameter $\xi^* (> 0)$ explains an average frequency of occurrence of pits. Then, the entirely same discussion in the beginning of the previous section leads to an approximate distribution for $Al(T)$ when T is large. The density of $Al(T)$ is given by (20). To avoid confusion, we denote $Al(T)$ by a random variable Y.

The density of Y is given by

$$f_\theta (y) = \frac{k^k \left(\frac{y}{\eta} \right)^{\sqrt{k}/\sigma} \exp\left\{ -k \left(\frac{y}{\eta} \right)^{\frac{1}{\sigma\sqrt{k}}} \right\}}{\sigma \sqrt{k} \Gamma(k) y}, \tag{38}$$

where we put

$$\eta = \exp \mu^* = T^{\tau} \exp \varphi^*, \tag{39}$$

$$\mu^* = \varphi^* + \tau \log T, \tag{40}$$

$$\varphi^* = \log C^* + \tau \log \xi^*. \tag{41}$$

As for a treatment of φ^* in (39), if we have some covariates $z_j \left(j = 1, \ldots, q\right)$ that may influence the frequency of occurrence of pits, we incorporate them into φ^* such that $\varphi^* = \beta_0 + \beta_1 z_1 + \cdots + \beta_q z_q$ with parameters $\beta_j \left(j = 0, 1, \ldots, q\right)$, because the definition (41) of φ^* includes parameter ξ^*, which describes the average frequency of occurrence of pits.

Analysis of accelerated testing data

So far, our investigation of Al cans filled with some drink shows that if those Al cans are made in an ordinary manufacturing process under control, Al dissolution seldom occurs even when one or two years have passed. Thus, we need an accelerated test to examine

the accumulated quantity of Al dissolution due to the elapse of time. Here we give two examples of accelerated tests in which we used Al cans with positive ERV as well as zero ERV. In the following two accelerated tests ERV is measured separately with respect to the lid and body of an Al can, and their values are sample averages with respect to lids and bodies that belong to the same lots.

Accelerated test 1 (*ERV>0*)

Factors of the accelerated test 1 are a type of contents $(=z_1)$ (two levels: carbonated or not), the position of an Al can $(=z_2)$ (two levels: the end is upward or downward), the temperature $(=z_3)$ (two levels: 25°C, 37°C), ERV of the body $(=z_4)$, ERV of the end $(=z_5)$ and the elapse of time $(=T)$ (the number of days).

Under the above conditions the accelerated test 1 was carried out for six months, and the accumulated quantity of Al elution was examined through the destruction of Al cans every one month. We applied our model (38) to the collected data (a sample size = 195). The predictor we picked is $\eta = \exp \mu^*$ with

$$\mu^* = \beta_0 + \beta_1 z_1 + \beta_2 z_2 + \beta_3 z_3 + \beta_4 z_4 + \beta_5 z_5 + \tau \log T ,$$

where categorical variables are

$$z_1 = \begin{cases} 1 & (carbonated) \\ 0 & (not\ carbonated) \end{cases}$$

$$z_2 = \begin{cases} 1 & (the\ end\ is\ upward) \\ 0 & (the\ end\ is\ downward) \end{cases}.$$

As for ERV of the end $(=z_5)$, when the end is upward, we need not take account of it. So we put

$$z_5 = \begin{cases} 0 & (z_2 = 1) \\ ERV\ of\ the\ end & (z_2 = 0) \end{cases}.$$

The result of our analysis is shown in Table 8. Similarly, in Table 8 we give the result when we applied our new power normal family (22) with the same predictor. In Table 8 we set $\hat{\beta}_4 = 0$, because ERV of the body $(=z_4)$ was not significant at all. The other estimates of regression parameters are all highly significant. These facts indicate that Al dissolution, in an Al can filled with some drink, is apt to arise when the Al can is put in the high temperature with the end being downward. As for ERV, Al dissolution is depressed when we make ERV of the end small.

Using the selected factors in Table 8, in case of $k = 1$ (i.e. the model (38) is the Weibull) we examined the minimum value (=SSE, shortly) of the negative log-likelihood function. Then, we have SSE=-121.89 and the p-value of a χ^2 test statistic is p=0.0115.

We also examined the case of k =100 (i.e. the model (38) is the Lognormal). We obtain SSE=-122.76 and the p-value of a χ^2 test statistic is p=0.0312. The distribution of the accumulated quantity of Al elution seems neither the Weibull nor the Lognormal.

To check the degree of the goodness-of-fit, we examine residuals

$$\hat{r} = \frac{\log y - \hat{\mu}^*}{\hat{\sigma}} \quad \text{and} \quad \hat{e} = \frac{1}{\hat{\delta}} \left\{ \left(\frac{y}{\hat{\eta}} \right)^{\hat{\delta}/\hat{\sigma}} - \exp\left(-\hat{\delta}^2\right) \right\}$$

of the model (38) and our new power normal family (22) respectively. The distribution of $\hat{r}$ is supposed to be the Gamma distribution with shape parameter $\hat{k}$, and so we give its Gamma probability plot in Figure 9. We also give a normal probability plot of $\hat{e}$ in Figure 9. Both probability plots show no peculiarity, but they suggest the existence of a small outlier.

Table 8

Figure 9

Accelerated test 2 (*ERV=0*)

Factors of the accelerated test 2 are a type of contents $(= z_1)$ (three levels: carbonated, weakly carbonated or not carbonated), the position of an Al can $(= z_2)$ (two levels: the end is upward or downward), the temperature $(= z_3)$ (three levels: 5°C, 20°C, 37°C), and the elapse of time $(= T)$ (the number of days).

Under the above conditions the accelerated test 2 was carried out for one year, and the accumulated quantity of Al dissolution was examined through the destruction of Al cans at the time when one, two, three, six and twelve months had passed. We applied the model (38) to the collected data (a sample size = 362). The predictor we picked is $\eta = \exp \mu^*$ with

$$\mu^* = \beta_0 + \beta_1 z_1 + \beta_2 z_2 + \beta_3 z_3 + \tau \log T,$$

where the categorical variable z_2 is the same in the accelerated test 1, but as for z_1 during the process of our analysis we found that we can put the *weakly carbonated* and *not carbonated* groups into one group. Thus, we put

$$z_1 = \begin{cases} 1 & (carbonated) \\ 0 & (weakly\ carbonated, not\ carbonated) \end{cases}.$$

We note that kinds of contents in Al cans are entirely different in the two accelerated tests. The result of our analysis is given in Table 9. The estimates of regression coefficients are all highly significant. In case of $k = 1$ (i.e. the model (38) is the Weibull), we have SSE=-743.87, which denies the null hypothesis: $k = 1$. Alternatively, in case of

k=100 (i.e. the model (38) is the Lognormal), we have SSE=-742.35, which denies again the null hypothesis: k=100.

Similarly, in Table 9 we give the result when we applied our new power normal family (22) with the same predictor. To check the degree of the goodness-of-fit with respect to both distributions (38) and (22), we also give probability plots for residuals in Figure 10. No singularity appears in both probability plots, but they suggest the existence of a large outlier.

Table 9

Figure 10

Finally we give some remark about estimation of the parameter k in the generalized Gamma distribution (38) (or (20)). It is well known that the convergence rate of an estimate of k is often very slow, and that sometimes its estimate does not converge. On the other hand, an estimate of the shape parameter δ in our new power normal family (20), which is a competitor against the generalized Gamma distribution (38), always converges. In our case study they seem to have the same performance. Thus, our new power normal family (20) can be always used to analyze the accumulated quantity of Al dissolution in Al cans.

Conclusions

We summarize several conclusions on this research. Our experimental study on ERV shows the following facts:

- ERV is proportional to $(defect\ size)^{\tau}$, and Al dissolution rate from defective areas is also proportional to ERV.
- The distribution of ERV data is the Weibull when sizes of defective areas are known.

Examination of six ERV data sets in real fields shows the following fact:

- When sizes of defective areas are unknown, ERV data with respect to bodies of Al cans follows, apart from the situation with a positive mass at the origin, the distribution $F_{\theta}(x)$, which is constructed by the Weibull with its scale parameter being distributed as a Gamma distribution. As for ERV data with respect to ends of Al cans, its distribution deviates from $F_{\theta}(x)$ in the upper tail.

Using the property of Al dissolution rate in the above first paragraph, we can derive

the distribution of accumulated quantities of Al dissolution in Al cans filled with some drink, of which functional form is some version of a generalized Gamma distribution. Statistical analyses of accelerated testing data on the accumulated quantity of Al dissolution in Al cans lead to the following conclusion:

- Performance of our generalized Gamma distribution is very good, but there is a serious problem in parameter estimation. Thus, instead of this generalized Gamma distribution a new power normal family is recommended for a practical use.

References

Box, G.E.P. & Cox, D. R. (1964) An analysis of transformation, *Journal of Royal Statistical Society*, B, 26, pp. 211-252.

Isogai, T. (1999) Power transformation of the F distribution and a power normal family, *Journal of Applied Statistics*, 26, pp. 355-371.

Isogai, T., Katano, Y. & Miyata, K. (2004) Models and Inference for Corrosion Pit Depth Data, *Extremes*, 7, pp.253-270.

Johnson, N. L. & Kotz, S. (1970) *Continuous Univariate Distributions*, Vol.1 (Wiley-Interscience).

Lawless, J. F. (1980) Inference in the Generalized Gamma and Log Gamma Distributions, *Technometrics*, 22, pp.409-426.

Lopez, A. (1987) *A COMPLETE COURSE IN CANNING AND RELATED PROCESSES, BOOK II-PACKAGING; ASEPTIC PROCESSING; INGREDIENTS*-, 12th Edition (The Canning Trade Inc).

Nishiyama, S. (1988) Corrosive Protection for All Aluminium Can, Boshoku Gijutsu, 37, pp. 578-579 (in Japanese).

Nishiyama, S., Kuribara, S. & Tohma, K. (1994) A Study of the Detection and Determination of Micro-Defects of All Aluminium Can Coating, *Zairyo-to-Kankyo*, 43, pp. 11-17 (in Japanese).

Prentice, R. L. (1975) Discrimination among some parametric models, *Biometrika*, 36, pp.202-232.

Table 1. Defect Count for each Defect Size

Defect Size (mm^2)	Unit Defect Size 0.0314 (mm^2)	Unit Defect Size 0.0628 (mm^2)	All
0.2	6.4	3.2	1
0.4	12.7	6.4	1
0.6	19.1	9.5	1
0.8	25.5	12.7	1
1	31.8	15.9	1
2	63.7	31.8	1
4	127.3	63.7	1
6	191.0	95.5	1
8	254.6	*	1
10	*	*	1
20	*	*	1

Note. (1) Defect Count = (Defect Size)/(Unit Defect Size)

(2) 'All' means a situation where Defect Size itself is Unit Defect Size.

Table 2. Analysis of ERV data with respect to

Box & Cox power normal family and a normal error model

Normal Error Model	Box and Cox Family
SSE = 316.06	SSE = 311.77
d.f. = 76	d.f. = 75
$\hat{\alpha}_1$ = 2.9815	$\hat{\alpha}_1$ = 2.8385
$\hat{\tau}_1$ = 0.5230	$\hat{\tau}_1$ = 0.5511
$\hat{\sigma}$ = 13.222	$\hat{\sigma}$ = 0.6331
	$\hat{\lambda}$ = 0.6358

(SSE = The minimum value of a negative log likelihood)

Table 3. Analysis of ERV/(defect count) with respect to Box & Cox power normal family and a normal error model

Normal Error Model	Box & Cox family
SSE = 237.88	SSE = 173.10
d.f. = 76	d.f. = 75
$\hat{\alpha}_2 = 2.6810$	$\hat{\alpha}_2 = 2.3903$
$\hat{\tau}_2 = 0.6262$	$\hat{\tau}_2 = 0.8613$
$\hat{\sigma} = 4.9149$	$\hat{\sigma} = 0.8338$
	$\hat{\lambda} = 0.4080$

(SSE = The minimum value of a negative log likelihood)

Table 4. Analysis of ERV data with respect to a generalized Gamma distribution and a new power normal family

Generalized Gamma	New Power Normal
SSE = 314.53	SSE = 316.06
d.f. = 75	d.f. = 75
$\hat{\alpha}_1 = 3.146$	$\hat{\alpha}_1 = 2.384$
$\hat{\tau}_1 = 0.5256$	$\hat{\tau}_1 = 0.5512$
$\hat{\sigma} = 0.5600$	$\hat{\sigma} = 0.8451$
$\hat{k} = 0.4631$*	$\hat{\delta} = 0.5374$

(* $\hat{k}$ did not converge.)

(SSE = The minimum value of a negative log likelihood)

Table 5. Analysis of ERV/(defect count) with respect to a generalized Gamma distribution and a new power normal family

Generalized Gamma	New Power Normal
SSE = 173.87	SSE = 173.12
d.f. = 75	d.f. = 75
$\hat{\alpha}_2 = 2.6901$	$\hat{\alpha}_2 = 2.0009$
$\hat{\tau}_2 = 0.8450$	$\hat{\tau}_2 = 0.8617$
$\hat{\sigma} = 0.7399$	$\hat{\sigma} = 0.9975$
$\hat{k} = 0.7409$	$\hat{\delta} = 0.3987$

(SSE = The minimum value of a negative log likelihood)

Table 6. Summary statistics of six ERV data sets with respect to bodies and ends of Al cans coming from ordinary manufacturing processes under control

Data set	A(H)	A(L)	B(H)	B(L)	E(H)	E(L)
Sample size	500	500	500	500	1425	480
Mean	0.0628	8.6008	0.1188	4.1802	0.3553	1.0704
Median	0	0	0	1.6	0.18	0.155
Standard Deviation	0.4323	13.537	0.2989	7.0199	0.7296	2.2678
Skewness	9.8429	2.7699	6.0401	3.3782	11.749	6.4509
Kurtosis	118.17	12.723	49.570	14.420	191.12	72.202
Minimum value	0	0	0	0	0.01	0
Maximum value	6.5	103.4	3.3	51.7	14.37	31.8
n_0 (the number of zero)	477	260	314	29	0	26
K (threshold value)	0.1	0.1	0.1	0.1	0.01	0.01

Note. A and B mean Al bodies made in Japanese factories, and H and L mean their uses for drinks of relatively high (H) and low (L) corrosiveness respectively. E means Al ends, and E(H) and E(L) are made in Japan and U.S.A. respectively.

Table 7. Analysis of six investigation ERV data sets

Data set	Estimators	Index of good coating (IGC)
A(L)	SSE = 1267.84 $\hat{p} = 0.480481$ $\hat{m} = 1.32345$ $\hat{\alpha} = 14.6774$ $\hat{\beta} = 0.288455$	1.001
A(H)	SSE = 116.288 $\hat{p} = 0.999992$ $\hat{m} = 4.33059$ $\hat{\alpha} = 0.00280371$ $\hat{\beta} = 0.000350793$	21.74
B(L)	SSE = 1167.55 $\hat{p} = 1$ $\hat{m} = 0.900952$ $\hat{\alpha} = 1.24465$ $\hat{\beta} = 0.371811$	1.062
B(H)	SSE = 197.057 $\hat{p} = 1$ $\hat{m} = 0.831385$ $\hat{\alpha} = 2.25845$ $\hat{\beta} = 13.6389$	2.688
E(L)	SSE = 311.546 $\hat{p} = 1$ $\hat{m} = 0.672168$ $\hat{\alpha} = 1.22609$ $\hat{\beta} = 1.57319$	1.057
E(H)	SSE = -161.165 $\hat{p} = 1$ $\hat{m} = 1.26508$ $\hat{\alpha} = 1.89436$ $\hat{\beta} = 6.52792$	1.000

(SSE = The minimum value of a negative log likelihood)

Table 8. Analysis of accelerated test-1 data

Generalized Gamma	New Power Normal
SSE = -125.08	SSE = -125.01
d.f. = 187	d.f. = 187
$\hat{\beta}_0$ =-5.0004	$\hat{\beta}_0$ = -5.1645
$\hat{\beta}_1$ = -1.6824	$\hat{\beta}_1$ = -1.6793
$\hat{\beta}_2$ = -0.6019	$\hat{\beta}_2$ = -0.5975
$\hat{\beta}_3$ = 0.04313	$\hat{\beta}_3$ = 0.04321
$\hat{\beta}_4$ = 0	$\hat{\beta}_4$ = 0
$\hat{\beta}_5$ = 0.1140	$\hat{\beta}_5$ = 0.1146
$\hat{\tau}$ = 0.4912	$\hat{\tau}$ = 0.4931
$\hat{\sigma}$ = 0.4462	$\hat{\sigma}$ = 0.4706
$\hat{k}$ = 4.1563	$\hat{\delta}$ = 0.1598

(SSE = The minimum value of a negative log likelihood)

Table 9. Analysis of accelerated test-2 data

Generalized Gamma	New Power Normal
SSE = -750.08	SSE = -750.28
d.f. = 355	d.f. = 355
$\hat{\beta}_0$ =-5.1317	$\hat{\beta}_0$ = -5.1645
$\hat{\beta}_1$ = 0.1806	$\hat{\beta}_1$ = 0.1831
$\hat{\beta}_2$ = -0.2147	$\hat{\beta}_2$ = -0.2174
$\hat{\beta}_3$ = 0.01087	$\hat{\beta}_3$ = 0.01096
$\hat{\tau}$ = 0.4995	$\hat{\tau}$ = 0.4969
$\hat{\sigma}$ = 0.5209	$\hat{\sigma}$ = 0.5614
$\hat{k}$ = 3.0226	$\hat{\delta}$ = 0.2012

(SSE = The minimum value of a negative log likelihood)

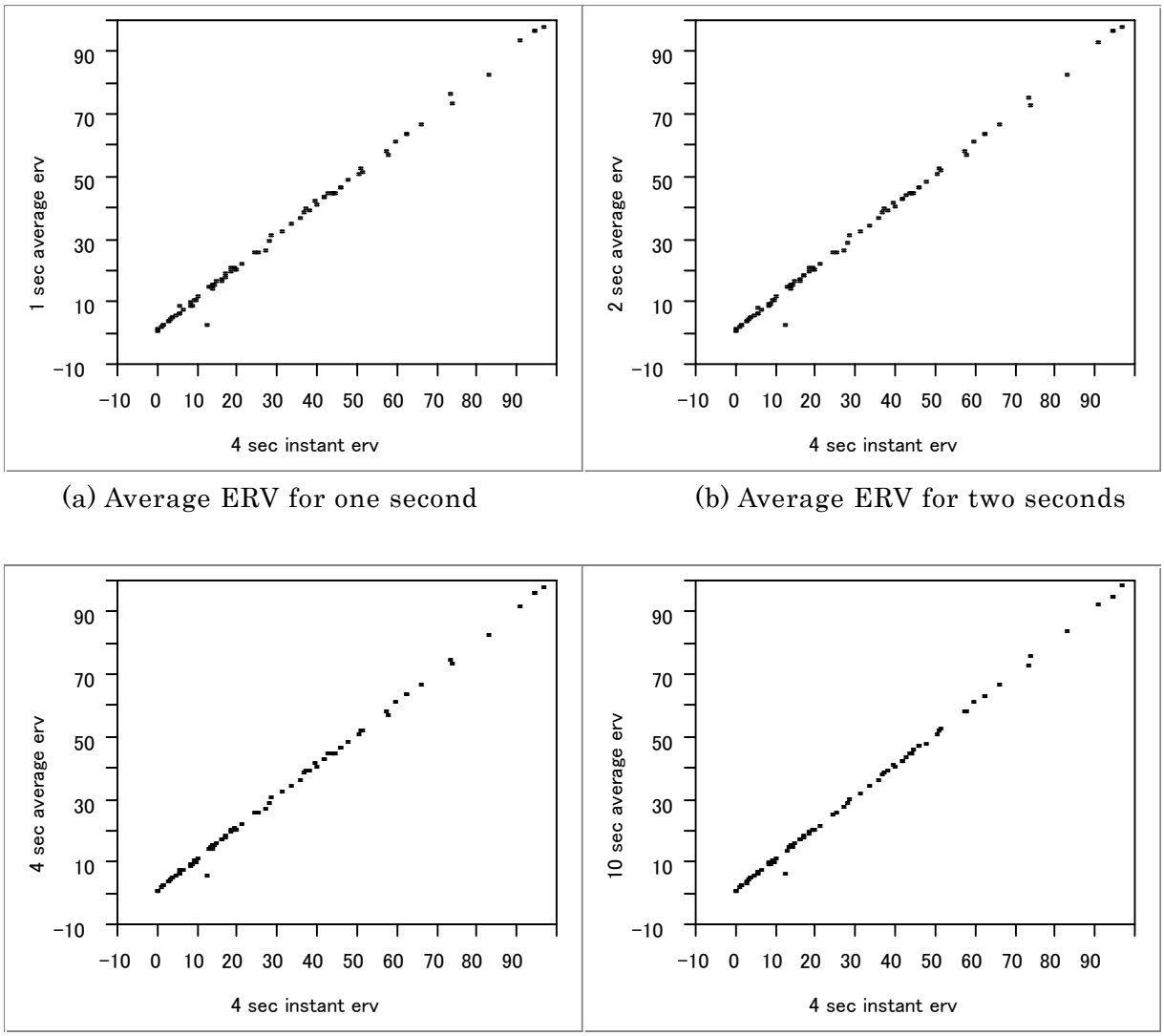

(a) Average ERV for one second

(b) Average ERV for two seconds

(c) Average ERV for four seconds

(d) Average ERV for ten seconds

Figure 1. Scatter plots between ordinary ERV, which is an instantaneous ERV after four seconds have passed from the beginning of measurement, and average ERV's for one, two, four and ten seconds.

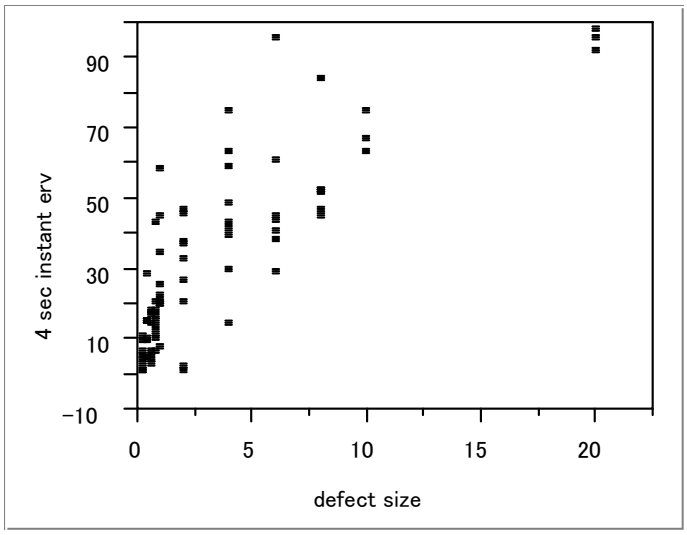

(a) Scatter plot between ERV and defect size

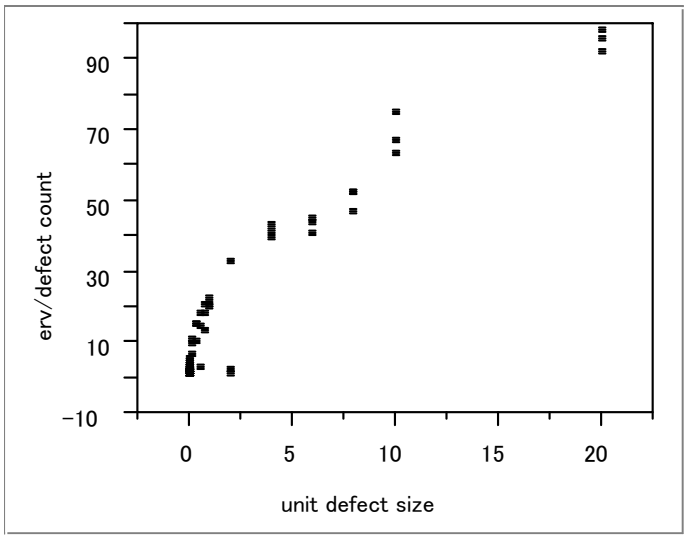

(b) Scatter plot between ERV/(defect count) and unit defect size

Figure 2. Relationship between ERV and defect sizes

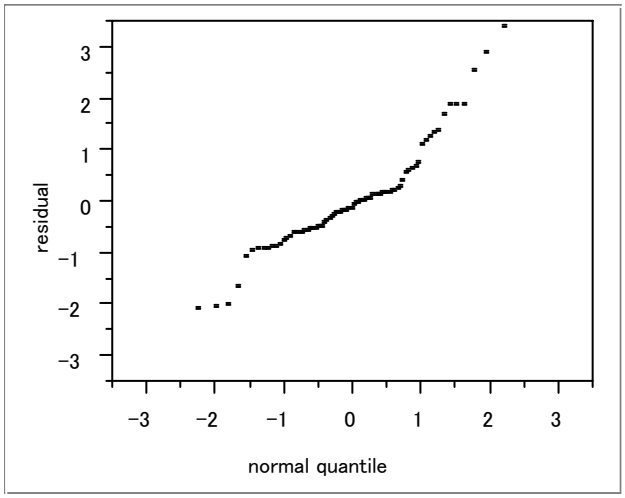

(a) Normal error model

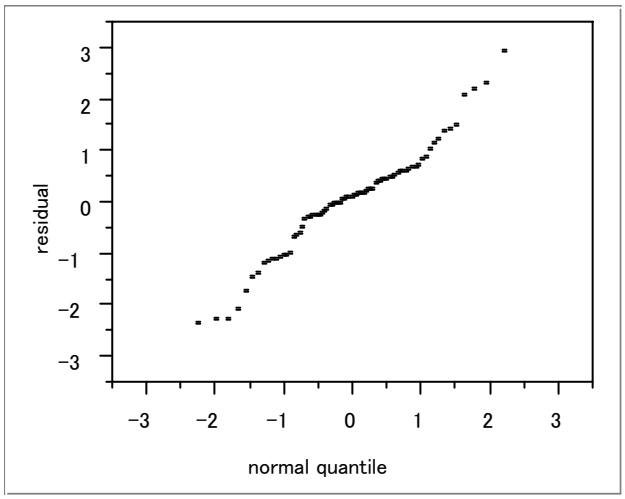

(b) Box & Cox power normal family

Figure 3. Residual plots of ERV data with respect to Box & Cox power normal family and a normal error model

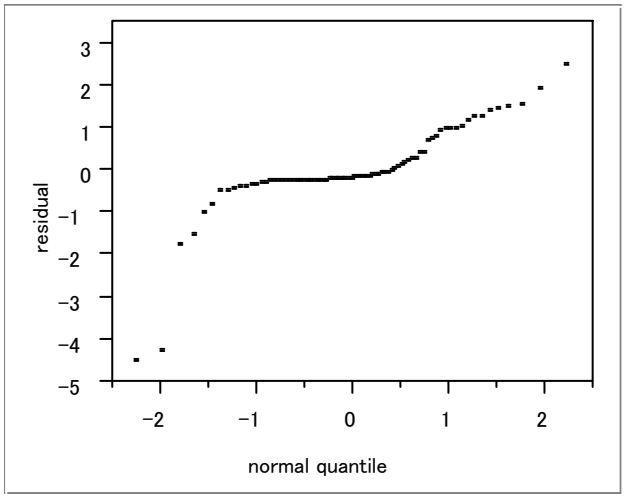

(a) Normal error model

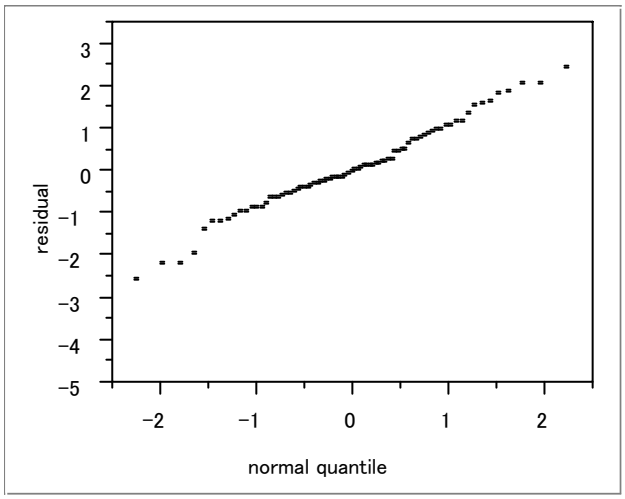

(b) Box & Cox power normal family

Figure 4. Residual plots of ERV/(defect count) with respect to Box & Cox power normal family and a normal error model

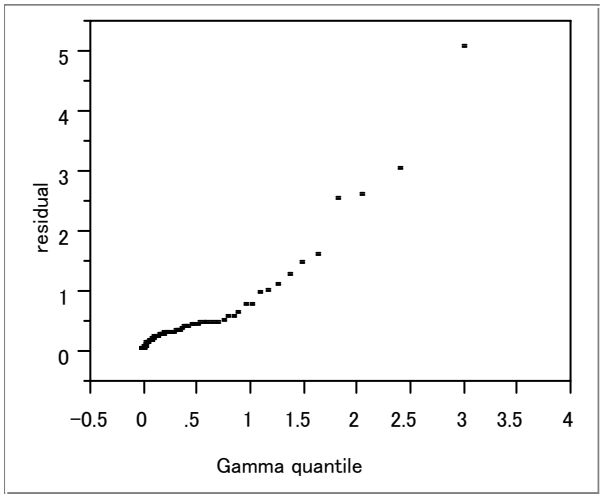

(a) Generalized Gamma distribution

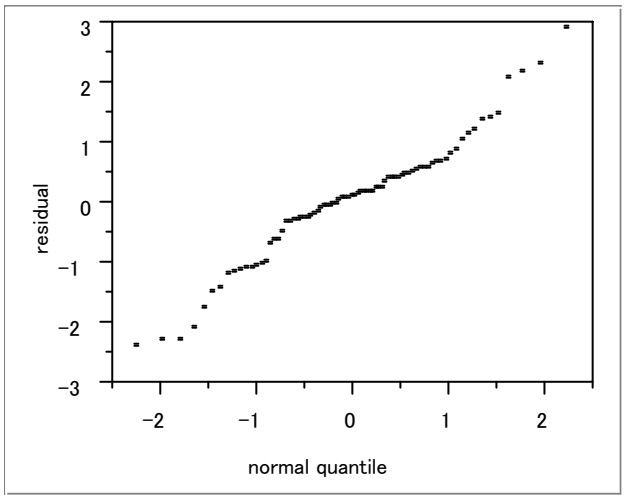

(b) New Power Normal Family

Figure 5. Residual plots of ERV data with respect to a generalized Gamma distribution and a new power normal family

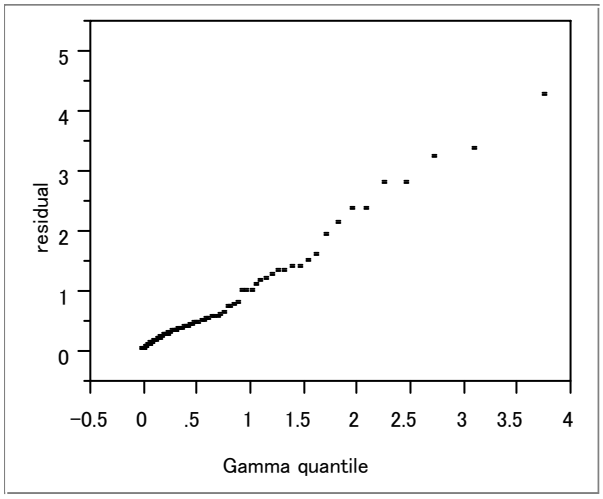

(a) Generalized Gamma distribution

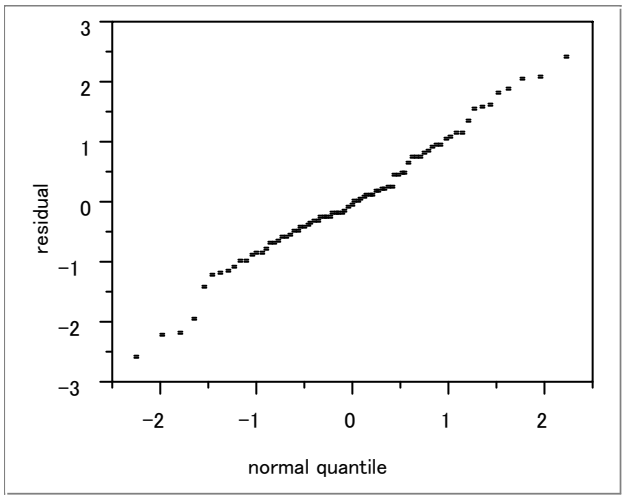

(b) New Power Normal Family

Figure 6. Residual plots of ERV/(defect count) data with respect to a generalized Gamma distribution and a new power normal family

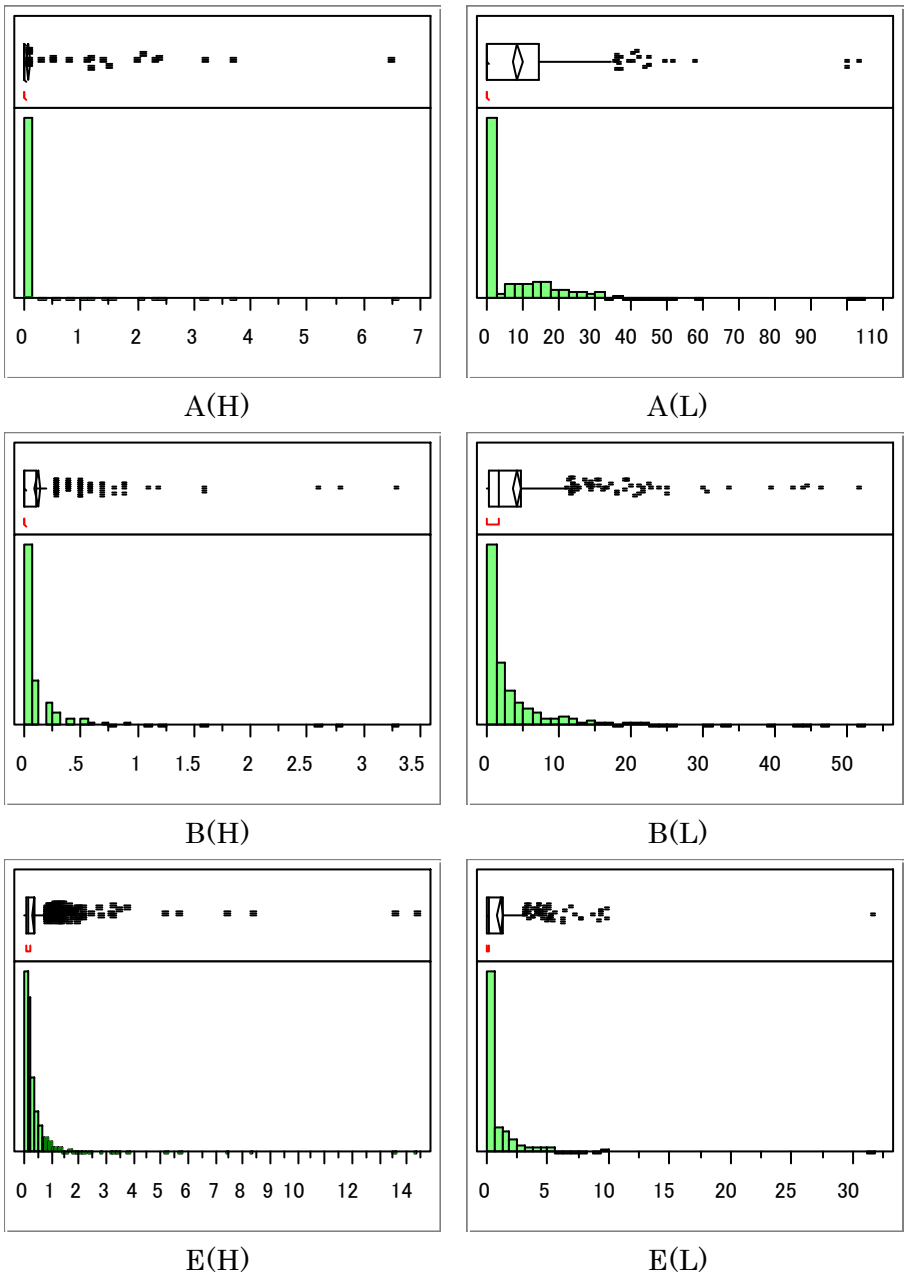

Figure 7. Histograms of six ERV data sets

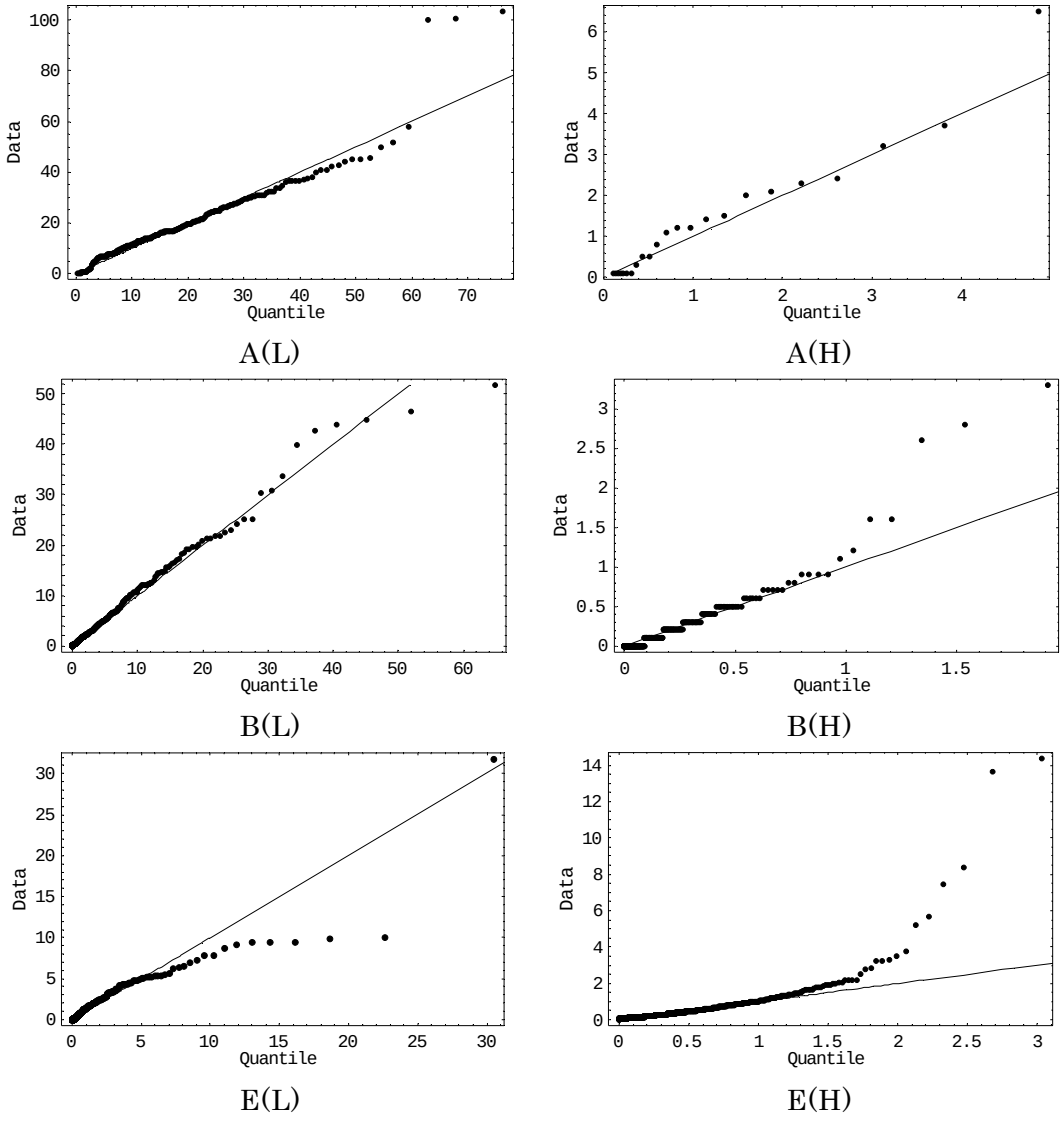

Figure 8. Probability plots of six ERV data sets

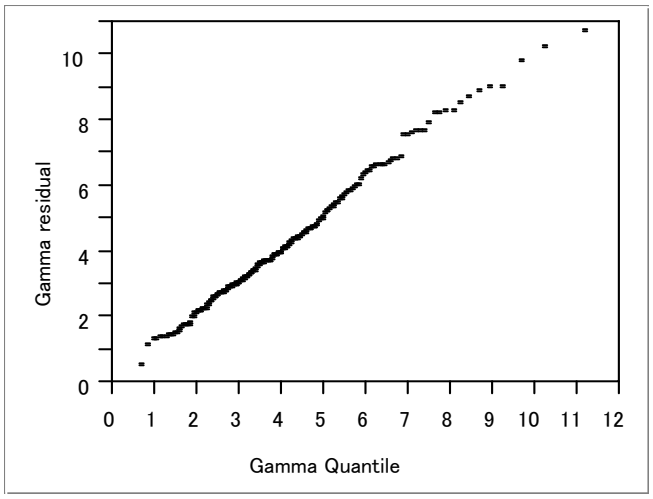

(a) Generalized Gamma

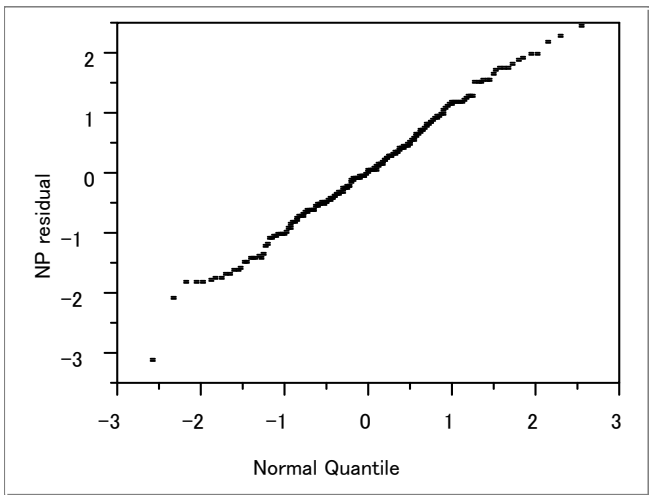

(b) New Power Normal

Figure 9. Residual plots for accelerated test-1 data

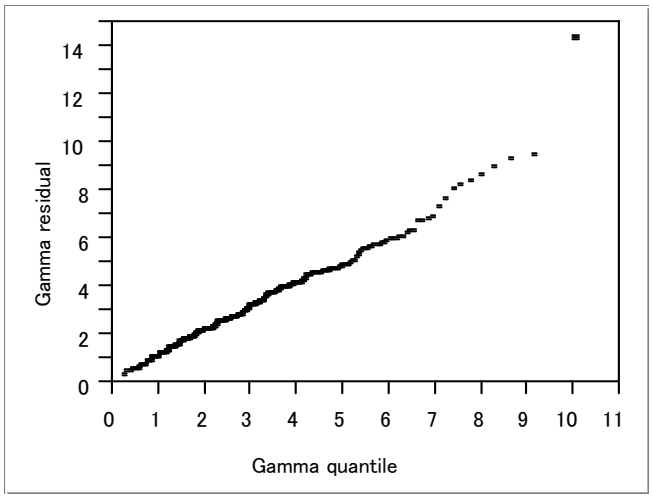

(a) Generalized Gamma

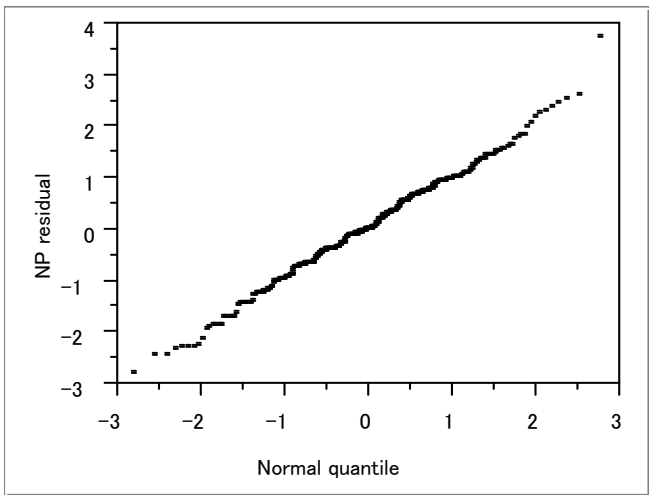

(b) New Power Normal

Figure 10. Residual plots for accelerated test-2 data